Dynamic Soil Pressures Caused by Travelling Forest Machines

Milan Marusiak, Jindřich Neruda

Abstract

Machines travelling in forest stands cause dynamic loading of soil, the size of which depends on a multitude of factors such as terrain ruggedness, machine speed, axle load and tyre inflation pressure. To decide on harvesting and transport machines suitable for specific field conditions, it is necessary to have at least some awareness about their dynamic effects on the soil, which sometimes considerably differ from static values measured on standing machines. The paper deals with the method of determining dynamic ground pressures according to the given parameters of vehicle weight and speed. At the same time, it compares dynamic pressures calculated by using this method with actually measured values.

Keywords: dynamic soil pressures, tyre deformation, contact area

1. Introduction

The travel of harvesters and forwarders across forest stands results in the contact occurring between the vehicle chassis and the ground surface. Machine weight and traction effects of the machine chassis induce ground pressures, which spread to sides and into depth. In wheeled machines, the ground pressures are influenced primarily by tyre characteristics such as diameter, width, rate (stiffness) and inflation pressure, other important parameters being adhesion load on the tyre and components of traction forces acting on the wheel. The vehicle contact pressure is the ratio between the weight and contact surface of the vehicle with the ground (soil), and it expresses the environmental suitability of a specific forest vehicle (Poršinsky et al. 2011).

Ground pressure is also considerably affected by characteristics of the soil surface across which the machine travels – elasticity and plasticity in particular. The effects of elasticity and plasticity especially show when the machine moves, the elastic soil returns to the original condition after temporary compression, and the wheel is also propped in the space behind the axis. The machine travelling across the plastic soil causes permanent deformation of the latter and the wheel is only supported by a part of the contact area. The value of instantaneous wheel load is also affected by the dynamics of machine travel including the dynamic effects of travelling across surface irregularities, where individual wheels experience higher load for a short time, and the wheel engagement may for a short time increase its power load (Neruda et al. 2013). The dependence of the tyre and soil contact area on elastic deformations of the loaded wheel (tyre characteristics, air pressure) and plastic-elastic soil deformations (granulometric content, moisture) is considered as problem when calculating the vehicle contact pressures for forest off-road travel (Poršinsky et al. 2011).

The soil profile, which generates the vibration of the vehicle, is significantly modified by the vehicle itself. The soil is compressed by the vehicle and part of the kinetic energy of the vibrating vehicle is absorbed by the soil, while the dynamic normal and shear forces affect the interaction. The dynamic load created by the moving tractor modifies soil cohesion significantly, while internal friction is not affected. The amount of change in cohesion is a function of travel velocity, the mass of the vehicle and moisture content (Laib 1999).

The total mass of the vehicle, the wheel load and dynamic shear forces are important factors affecting the degree of soil deformation. During soil compaction, strength and bulk density increase, porosity is reduced, the pore size distribution changes, and the infiltration rate decreases (Greacen and Sands 1980).

The extent of soil degradation by farm tractor forwarding operations along the upper 20 cm of the soil profile increase with traffic frequency, but these increases vary with slope gradient and direction of forwarding (Jourgholami et al. 2014).

Actual ground pressures, particularly in the upper soil layers, up to a depth of 15 cm, where a majority of spruce root systems occur, presumably differ from static pressures established by calculation. Therefore, it is necessary to know the actual values of ground pressures in order to be able to compare the impact of travelling forest machines on the condition of the root system. Saarilahti and Antilla (1999) consider the soil layer at a depth of 15 cm as the most representative in terms of the agreement of measured and calculated data of penetration soil resistance.

The paper presents a method of calculating dynamic ground pressures according to the given parameters of vehicle weight and speed, which is based on an assumption that the dynamic wheel load is build on the law of energy conservation and transformation on impact.

The calculated dynamic pressures are compared with the results from measuring the direct ground pressures of eight-wheeled forwarder L511 with max. payload of 5 t.

1.1 Used symbols

- b tyre width, m
- b_c tyre contact width, m
- b_w tyre tread pattern width, m
- β dynamic coefficient
- d tyre diameter, m
- δ tyre deformation, m
- δ_{st} static tyre deformation, m
- δ_r tyre deformation at static load, m
- F_d dynamic load on the wheel, N
- F_k static load on the wheel, N
- F_n nominal load on the wheel, N
- G_v vehicle weight load, kN
- g gravitational acceleration, m×s^{-2}
- h tyre profile height, m
- k tyre rate, stiffness, N×m^{-1}
- k_2 constant taking into account the number of driving axles 2.05–4 axles, 1.95–3 axles and 1.83–2 axles
- l_c tyre contact length, m
- K kinetic energy, J
- m vehicle weight proportion per tyre, kg
- n number of axles,
- p contact ground pressure, kPa
- p_d contact ground pressure at dynamic load, kPa
- p_i tyre inflation pressure, kPa
- r unloaded tyre radius, m
- r_s tyre static radius, m
- S tyre contact surface area (print), m^2
- v vehicle speed, m×s^{-1}
- U potential energy, J
- U_r potential energy of stress, J
- z wheel sinking (rut depth), m

2. Theoretical Analysis

2.1 Contact ground pressure

There are many authors dealing with the determination of contact ground pressure. The simplest calculation of contact ground pressure is given by its definition as a ratio of the wheel load and the tyre contact area – see for example Pacas et al. (1990):

$$p = \frac{F_k}{S} \quad (1)$$

In practice, a simple estimate of vehicle crossing ability in certain soil conditions is often made by using the NGP (Nominal Ground Pressure) method (Partington and Ryans 2010), according to which contact ground pressure is expressed by the following relation:

$$p = \frac{F_k}{b \times r} \quad (2)$$

According to this method, the length of the wheel contact with the ground equals the wheel radius, which presumes a wheel sinking in the ground at a depth of about 15% of its diameter. As compared with the measured contact pressure, the calculated contact pressure is too low and the sinking of a larger wheel represents a depth, which is not suggested for ecological reasons. Another disadvantage of this method is the negligence of important parameters of wheel contact with the ground such as tyre deformation and inflation pressure (Saarilahti 2002).

To compare the crossing capability of military tracked and wheeled vehicles on soils with low carrying capacity, a method was developed in the early 1970s for the determination of mean maximum contact ground pressure MMP (Rowland 1972). MMP (Mean Maximum Pressure) represents the mean value of maximum contact pressures by which the vehicle affects the soil when travelling. To provide vehicle mo-

bility, the soil carrying capacity must be greater than the MMP value for the given vehicle. This method was later worked out by more authors for various chassis configurations (wheeled, tracked, tracked on tandem axles) and soil conditions (cohesive soils and frictional soils).

The original formula for the calculation of contact pressure by using the MMP method (Rowland 1972) for off-road tyres is as follows:

$$p = \frac{1.18 \times G_v}{2 \times n \times b \times \sqrt{d \times h}} \quad (3)$$

Larminie (1992) elaborated modified formulas for calculating MMP, into which he also included tyre deformation as an important parameter. Contact pressure for wheeled vehicle on fine grained cohesive soils is calculated according to the following relation:

$$p = \frac{k_2 \times G_v}{2 \times nb^{0.85} \times d^{1.15} \times \sqrt{\frac{\delta}{d}}} \quad (4)$$

Building on the methodology of measuring soil carrying capacity by means of cone penetrometer, in which soil resistance is measured against cone penetration at a depth of 15 cm, Maclaurin (1997) suggested replacing the MMP value by the expression of Limiting Cone Index (CI_L). The measuring method is governed by the norm ASAE EP542 1999 and the gauged value of soil resistance is called Cone Index. Limiting cone index expresses the lowest load with respect to soil carrying capacity, at which the vehicle with a certain MMP is still mobile. According to this methodology, the contact pressure is calculated as follows:

$$p = \frac{1.18 \times G_v}{2 \times n \times b^{0.8} \times d^{0.8} \times \delta^{0.4}} \quad (5)$$

The above methods for determining contact pressure use static load of the vehicle as an input value. However, in actual conditions of machines moving within the forest stand, there are dynamic effects on the soil caused by machines passing over terrain irregularities that, in some cases, may be several times higher than their static values. A simple calculation of the static ground contact pressure of forest harvesting machines is not a good indicator of the dynamic pressure exerted on soil during skidding (Lysne and Burditt 1983). The ground contact pressure is not uniformly distributed over the contact area, and its distribution beneath the wheel is complex due to a number of variables, such as tyre lug pattern, tyre load distribution, and tyre carcass stiffness (Peng et al. 1994). The maximum ground contact pressure under lugs or stiff tyre sidewalls may be several (even ten) times higher than the estimated average ground contact pressure (Burt et al. 1992).

To be able to assess the impact of forest machines on the soil surface, it is therefore important to identify not only static but also dynamic forces acting in the mutual interaction of machine chassis and soil surface (Neruda et al. 2013). The mode by which the dynamic forces manifest themselves in specific conditions of given soil profile can be documented for example by measuring dynamic ground pressures.

Table 1 brings calculation formulas for establishing contact pressure, presented by several authors. None of the formulas mentioned in the literature is universally applicable for estimating the suitability of tyre use in soils with low carrying capacity. Saarilahti (2002) recommends using formulas with tyre deformation entered as an input variable because their results lead to a better choice of the tyre from the environmental point of view. Eq. (2) through to (6) use static wheel load as an input value. Eq. (1) expresses the value of contact pressure at dynamic load calculated according to the procedure given in Material and Methods, Fig. 3.

Table 1 Contact pressure – calculation formulas

Source	Calculation model	
	Equation	Number
Pacas (1990)	$p_d = F_d/S$	*(1)*
NGP	$p = F_k/r \times b$	*(2)*
MMP Rowland (1972)	$p = 1.18 \times F_k/(2 \times b \times (d \times h)0.5)$	*(3)*
MMP Larminie (1988)	$p = k_L \times F_k/2 \times b^{0.85} \times d^{1.15} \times (\delta/d)^{0.5}$ $k_L = 2.05$	*(4)*
MMP Maclaurin (1997)	$p = 1.85 \times F_k/2 \times b^{0.8} \times d^{0.8} \times \delta^{0.4}$	*(5)*
Dwyer (1984)	$p = (F_k/b \times d) \times (h/\delta)^{0.5} \times (1 + b/2 \times d)$	*(6)*

2.2 Static Tyre Deformation

One of important characteristics of the tyre is its rate (stiffness), which is expressed by the load/deformation ratio. Tyre rate depends on tyre design (diagonal or radial and number of layers), size and inflation pressure. If tyre rate data are not available from the manufacturer, the value can be determined based on the known load and deformation calculated in depen-

dence on tyre size and type, using empirical formulas published by several authors.

Table 2 brings empirical formulas for the calculation of tyre deformation presented by several authors, obtained from the processing of tyre deformations measured during the tests of forest and agricultural machines. The data express the dependence between tyre deformation, inflation pressure and load (possibly also size) and apply only to the dimensions of tyres used in the tests (within a certain range).

Table 2 Tyre deformation – calculation formulas

Source	Calculation formula	Number
Wulfsohn et. al (1988)	$\delta = 0.02+0.006\times F_d-1.35\times F_d\times p_i\times 10^{-5}$	*(7)*
Nokia, model 1	$\delta = 0.121\times F_d^{0.476}/p_i^{0.570}$	*(8)*
Nokia, model 2	$\delta = 0.008+0.001\times(0.365+170/p_i)\times F_d$	*(9)*
Godbole (1993)	$\delta = h\times 0.67\times(p_i\times d\times b/F_d)^{-0.8}$	*(10)*
Schmidt (1988)	$\delta = 0.01+(0.0007+0.302/p_i)\times F_d$	*(11)*

2.3 Determination of Dynamic Load

Passing through a rugged terrain, the forest machine chassis is exposed to the load the size of which constantly changes depending on the size of obstacles and terrain irregularities the machine has to cross. Since the terrain in the forest stand is not homogeneous, the forest machine tyre behaviour can be considered as a system under the influence of shock in order to simplify the calculation. In a system stressed in this way, the load size would change within a short time interval and its maximum value can be several times higher than the static load of the standing machine. The size of dynamic wheel load can be established based on the law of energy conservation and transformation on impact. Kinetic energy of the moving wheel, represented by its load and velocity, would change into potential energy of the flexible system stress, represented by the rate and deformation of the tyre (Fig. 1)

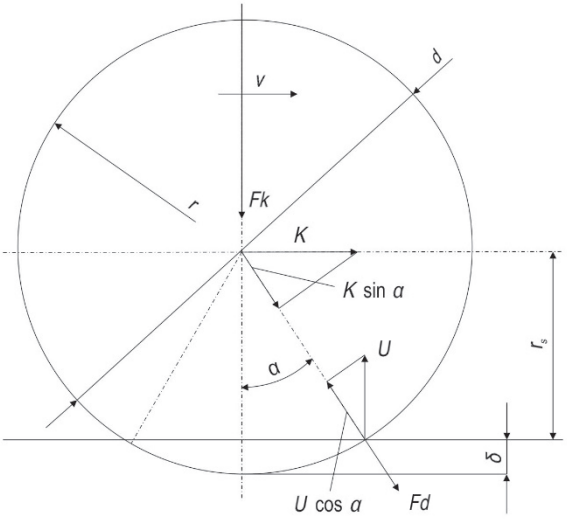

Fig. 1 Energies and forces on the rolling tyre

Kinetic energy (K) is expressed by the following formula (Zahradníček and Semrád 2007):

$$K = \frac{m\times v^2}{2},\ J \qquad (12)$$

Initial potential energy (U) is expressed by the following formula:

$$U = F_k\times\left(\frac{v^2}{2\times g}\times\delta_r\right),\ J \qquad (13)$$

This is changing into potential stress energy caused by tyre deformation upon the wheel contact with the base:

$$U_r = \frac{k\times\delta_r^2}{2},\ J \qquad (14)$$

Tyre rate can also be expressed as a ratio of load and deformation at static load as follows:

$$k = \frac{F_k}{\delta_{st}},\ Nm^{-1} \qquad (15)$$

Modifying the Eg. (12) through to (14) and taking into account α angle (Fig. 3), a formula for the calculation of dynamic deformation of the tyre is obtained:

$$\delta_r = \delta_{st}\times(1+\sqrt{1+\frac{v^2\times sin\alpha}{2g\times cos\alpha\times\delta_{st}}}),\ m \qquad (16)$$

The expression in brackets is called a dynamic coefficient (β) and gives the ratio of the increase of dynamic deformation δ_r compared to static deformation δ_{st}. It can be also expressed as:

$$\beta = 1+\sqrt{1+\frac{K}{U}} \qquad (17)$$

Pursuant to Hooke's Law, the force and stress are directly proportional to strain (deformation), and the below formula holds for the size of dynamic load F_d:

$$F_d = \beta \times F_k \, , \, N \qquad (18)$$

The following conclusions can be made based on the above relations (16), (17) and (18):

⇒ Increased static load and increased travel speed result in increased dynamic load

⇒ Increased elasticity of the tyre (e.g. due to decreased inflation pressure), which is expressed by increased static deformation and increased angle α, results in decreased dynamic coefficient β and hence in decreased dynamic load.

2.4 Tyre contact area

The forest machine chassis makes contact with the soil surface in the stand and the size of the contact area depends on several factors such as tyre dimensions, tyre deformation, inflation pressure, wheel load, and soil characteristics (soil texture, carrying capacity, moisture content) (Hallonborg 1996, Neruda et al. 2013). On the hard rigid basement (concrete, asphalt, paved road), the tyre contact area is smaller, its shape ranging from circular to rectangular in dependence on the tyre type and inflation. If the tyre sinks into the soil of low carrying capacity, tyre tread sides carry some load too, and the contact area is represented by the general area (Pacas et al. 1983). In practical calculations, the vertical projection of this general area is most frequently used as a contact area, or the tyre print area on the solid base.

The size of the tyre contact area is also affected by the machine dynamics, i.e. by the machine movement and by the engagement of its wheels. Low inflation pressure, high tyre load, and soft soils contribute to large contact areas. In forests, vehicles move on a plastic matrix composed of soil, thus producing an asymmetric contact area that is perpendicular to the tyre. If vehicles move laterally on a slope, the contact area of the wheels is asymmetrical with respect to the longitudinal axis. The size of the contact area changes continuously due accelerating/braking, changing payload, and uneven soil surface (Alakukku 1999).

The determination of the contact area has been dealt with by several authors, who developed calculation formulas based on observations and measured values.

Reviewing the shape of the contact area, Grecenko (1995) recommended multiplying the length and the width of the contact area by a coefficient, *c*, varying between 0.8 and 0.9.

Hallonborg (1996) proposed a super ellipse model to describe the geometry of tyre-terrain contact with half-axes, *a* and *b*, as well as a positive variable exponent to determine the shape of the ellipse. Nevertheless, they require input data that are not easily acquired, and do not consider the rapid dynamic variation during machine trips.

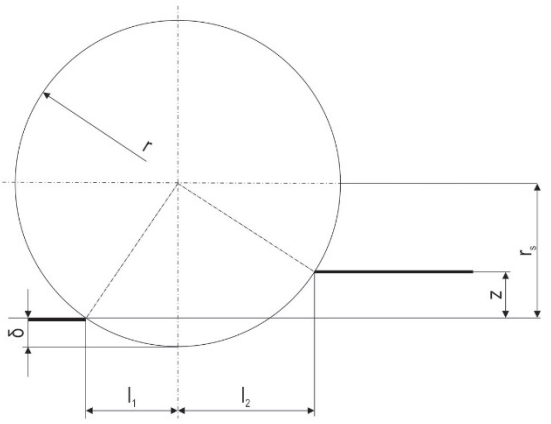

Fig. 2 Elastic tyre on soft ground

Analytical calculation formulas are based on the definition of loaded wheel geometry in interaction with the soil environment. The best simulation of the travel of forest machines in the terrain is the model, which describes elastic tyres on soft ground (Fig. 2). In this case, the deformation occurs of both the tyre and the ground.

The calculation formula for this case was elaborated by Schwanghart (1990) based on wheel geometry (Fig. 1). The tyre print area is calculated according to the following formula:

$$A = c \times b_c \times l_c \, , \, m^2 \qquad (19)$$

Where:

c constant, expressing the shape of tyre print. The tyre print shape depends on tyre design, inflation pressure, wheel load and soil characteristics. Its outer contour ranges between the circle and the rectangle. The value recommended for the tyres of forest machines is $c = \pi/4 = 0.785$

b_c contact width, m – is the maximum width of tyre print

l_c contact length, m – is the total length of tyre print. It consists of two contact lengths l_1 and l_2 (Fig. 2):

$$l_c = l_1 + l_2 = \sqrt{d \times (z + \delta) - (z - \delta)^2} + \sqrt{d \times \delta - \delta^2} \, , \, m \qquad (20)$$

One of the input parameters in the calculation of contact length is the depth of tyre sinking in the

Table 3 Tyre contact area – calculation formulas

Source	Calculation formula	Number
Schwanghart (1990)	$S = 0.785 \times b_c \times l_c$ $b_c = b + c.\ F_d/F_n$ [$c = 0.03...0.05$] $l_c = (d \times (z+\delta) - (z+\delta)^2)^{0.5} + (d \times \delta - \delta^2)^{0.5}$	*(21)*
Grecenko (1995)	$S = 1.57 \times (d - 2 \times r_s) \times (d \times b)^{0.5}$	*(22)*
Lyasko (1994)	$S = \pi/4 \times l_c \times b_c$ $l_c = c_3 \times (d \times \delta - \delta^2)^{0.5}$ $c_3 = 23/(ABS(d/b - 3.5) + 11.9)$ $b_c = 2 \times ((b + h/25) \times \delta - \delta^2)^{0.5}$	*(23)*
Febo (1987)	$S = \pi/4 \times b_c \times l_c$ $l_c = 2 \times d^{0.5} \times \delta^j$ [$j = 0.44$] $b_c = b_w(1 - exp^{-k.\delta})$ [$k = 36$]	*(24)*
Komandi(1990)	$S = (c_2 \times F_d^{0.7} \times (b/d)^{0.5})/p_i^{0.45}$	*(25)*
Dwyer (1984)	$S = F_d/G$ $G = F_d/b \times d \times (h/\delta)^{0.5} \times (1 + b/2 \times d)$	*(26)*

ground (z). Several ways of its determination, based on the WES method, are mentioned in literature (Maclaurin 1990). For simplification, values used in the following calculation are rut depths measured after the first pass of the forwarder Model L511 during the tests: loaded machine – $z = 0.08$ m; empty machine – $z = 0.07$ m.

Empirical calculation formulas were developed based on the observation of the dependence of tyre print size on tyre parameters (rate (stiffness) as expressed by strain (deformation), diameter, width, inflation pressure) and soil environment characteristics (soil texture, penetration resistance, moisture content) (Saarilahti 2002).

Empirical calculation formulas selected for further processing include the following input parameters: tyre dimensions and deformation, inflation pressure, wheel load, possibly also tyre sinking depth. Calculation formulas for the determination of the tyre contact area and their comparison with the measured values are presented in Table 3.

3. Material and methods

To be able to determine dynamic ground pressures, we first need to know the size of dynamic load by which the forest machine acts on the soil while travelling at a certain speed. The procedure for determining the dynamic load and dynamic ground pressures consists of the following issues:

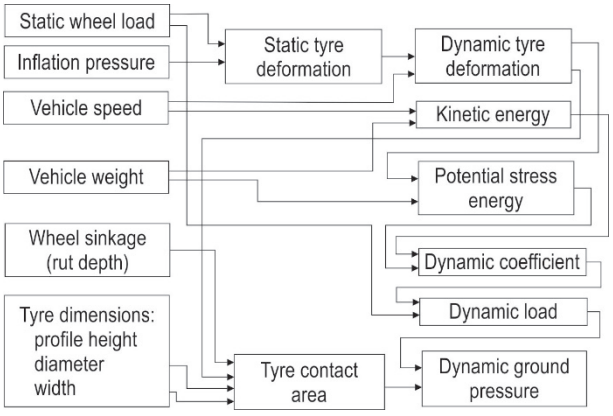

Fig. 3 Procedure for determining dynamic pressures

⇒ Determination of tyre deformation under static load. Based on the measured values of deformation, a relation for the calculation is established, which expresses the dependence of tyre deformation on tyre load (tyre rate) and inflation pressure.

⇒ Determination of dynamic wheel load in the machine moving at a certain speed on flat terrain by using the power conservation law.

⇒ Calculation of tyre/ground contact area at a given dynamic load. Comparison of calculation formulas developed by several authors and selection of a formula, the results of which are closest to the contact area values, measured during forwarder L511 trials.

⇒ Calculation of dynamic pressures at a given contact area and dynamic load; Comparison of measured dynamic axle pressures with values calculated according to dynamic load and according to calculation formulas presented by several authors. Determination of static/dynamic pressure ratios.

The correlation between the individual parameters in the procedure of determining the dynamic ground pressures is illustrated in Fig. 3 presented below.

3.1 Measurements of Dynamic Contact Pressures

Dynamic contact pressures were measured during tests conducted on the forwarder Model L511 in the locality of Maršov (Czech Republic). Researchers at the Faculty of Forestry and Wood Technology, Mendel University in Brno, developed a method for measuring and registering direct ground pressures by using a pressure probe installed at a shallow depth below the soil surface at the site of machine pass (Zemánek 2015).

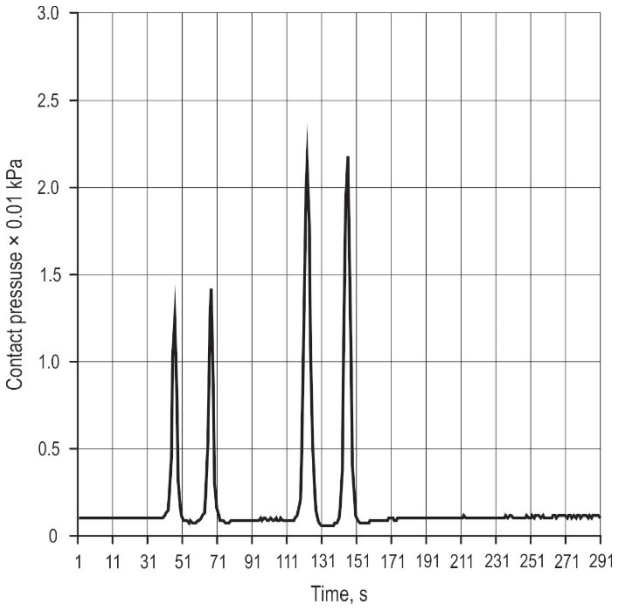

Fig. 4 The course of contact pressure during the forwarder pass

Dynamic pressures in the ground were measured by using the measuring equipment consisting of pressure sensor, which included a strain gauge connected to a pressure probe, a converter of analogue-digital signal, and a notebook with the measuring programme.

The system of pressure probe and strain gauge was filled with liquid and de-aerated. Thus, a homogeneous hydraulic connection was created, by which the ground pressure on the walls of the pressure probe was transferred to the sensor. The accuracy of the measuring equipment was regularly checked by loading the pressure probes with a defined burden, by subsequent reading of pressure values and by their comparison with the calculated results. The maximum measurement error was 5%. During the measurements, the pressure probe was installed in the soil at a depth of 20 cm. This depth was chosen because the zone contains a considerable amount of roots of shallow rooting trees that are exposed to damage during the passage of forest machines (Zemánek et al. 2015). The placement of the probe was followed by the measurement of 10 machine travels in the same rut (5 forward and 5 back) in the loaded and empty version.

Fig. 4 shows the course of contact pressure values recorded by the pressure probe during the second travel of the forwarder.

For comparing the calculated and measured values of dynamic pressure, data from the second through to fifth machine pass were used. The reason is that during the first pass, the measured pressure values are usually lower due to the clearance between the hole drilled in the soil and the diameter of the pressure probe (Zemánek 2015).

4. Results and Discussion

4.1 Tyre Deformation

In 2015, a series of measurements and tests of parameters of the 8x8 forwarder Model Novotny L511 (max. payload 5 t) were conducted at Mendel University in Brno. The tests also included the measuring of wheel static radius under different values of inflation pressure in tyres and load. Static radius was measured on the rear axle of the machine as a distance from the

Table 4 Measured average values of static radius and tyre deformation

Machine weight kg	Weight proportion per rear axle kg	Inflation pressure p_i, bar	Measured static radius r_s, m	Tyre deformation δ, m	Dispersion index
6220 (Empty machine)	2750 (Empty machine)	3.5	0.412	0.013	0.00024
		2.5	0.403	0.022	0.00027
		1.5	0.381	0.044	0.00058
10 920 (Loaded machine)	8570 (Loaded machine)	3.5	0.405	0.020	0.00020
		2.5	0.398	0.027	0.00028
		1.5	0.318	0.107	0.00041
Tyres					
Type		Diameter, m	Radius, m	Width, m	Profile height, m
Mitas D FOREST 400/60–15.5		0.85	0.425	0.405	0.24

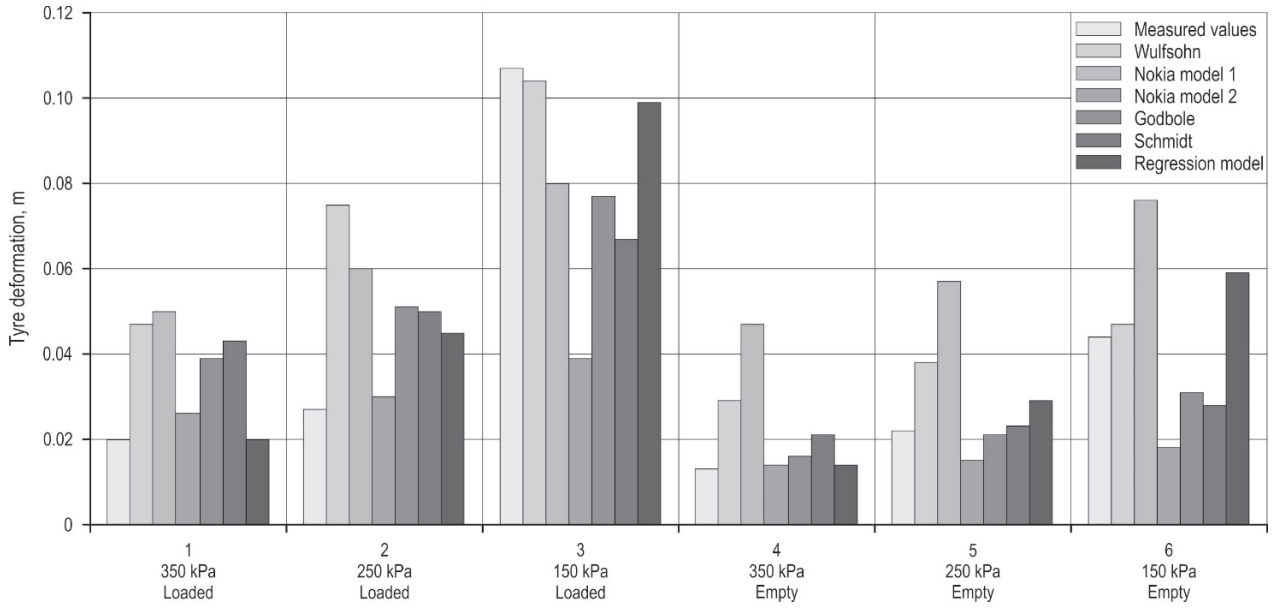

Fig. 5 Measured and calculated values of tyre deformation

centre of the wheel hub to the base surface. The difference between the measured static radius and the radius of unloaded tyre then represents the tyre deformation. Results of measurements and calculated values of tyre deformation of rear axle are presented in Table 4.

According to measured values of static radius the following formula for calculating the tyre deformation was developed through regression:

$$\delta = 0.001 \times F_{\mathrm{d}}^{\left(-0.008 \times p_{\mathrm{i}} + 0.577\right)}, m \qquad (27)$$

Fig. 5 presents the comparison of measured and calculated values of tyre deformation.

The agreement of measured and calculated data, expressed by correlation coefficient r^2, is presented in Table 5.

Table 5 Tyre deformation – correlation coefficients

Source	Calculation equation number	r^2
Wulfsohn et. al (1988)	*(7)*	0.853
Nokia, model 1	*(8)*	0.854
Nokia, model 2	*(9)*	0.764
Godbole (1993)	*(10)*	0.841
Schmidt (1988)	*(11)*	0.758
Formula developed through regression according to measured values	*(27)*	0.963

Even though the r^2 correlation coefficients between the measured and calculated tyre deformation values are relatively high, certain differences can still be observed in Fig. 5, especially in the loaded tyre.

The last equation (27), developed by using regression according to measured values of static wheel radius, where r^2 represents a value of 0.963, suits best the deformation of the tyre Mitas D FOREST 400/60–15.5. This formula is used in the following calculations of dynamic load and contact area of the tyre.

Tyre overloading beyond the tolerable limit can also be seen in Fig. 6, where the calculated curves of tyre deformation are illustrated in dependence on the load. Solid line represents tyre deformation curves at static load, while dashed line represents tyre deformation caused by the dynamic equivalent of static load during the machine travel. Horizontal lines illustrate the degree of tyre strain (deformation) at permitted tyre load and inflation pressure. The rear axle tyre of the loaded machine (F_{k}=15 900 N) is at the level of the limit deformation already under the static load. During the machine drive with underinflated tyres (150 kPa), the permitted deformation is already exceeded with the empty machine. In the loaded moving machine, the profile height of the rear axle tyre is so low that there is a risk that the tyre casing might come into contact with the tyre bead causing a sidewall collapse.

4.2 Tyre Contact Area

The contact surface of the forwarder tyre has been determined experimentally by measuring the external

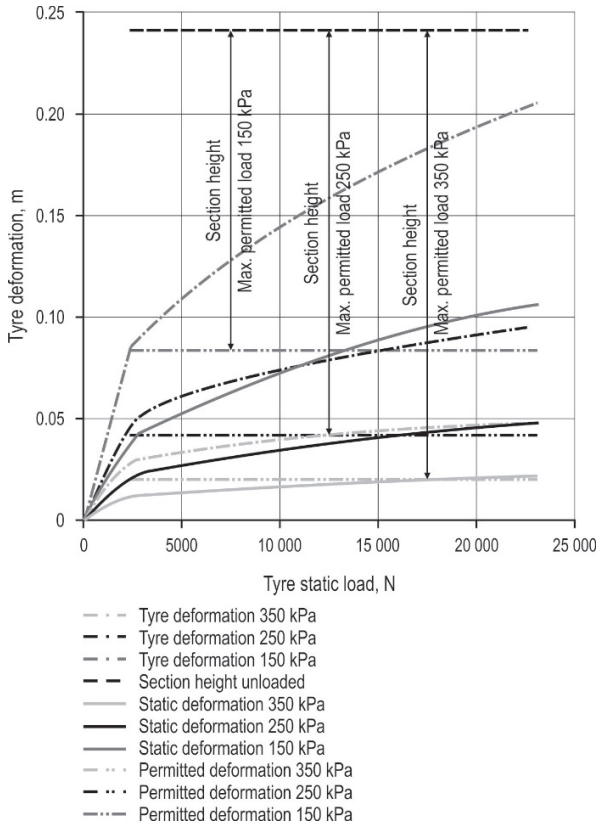

Fig. 6 Tyre deformation

dimensions of the tyre imprinted in the soil. These external dimensions were embedded in a rectangle, and the area of this rectangle was considered to simulate the tyre contact area. Measure values of the tyre contact area are presented in Table 6.

Table 6 Measured values of tyre contact area

Machine	Axle	Wheel load, N	Inflation pressure, kPa
			350
			Tyre contact area, m^2
Empty	Front axle	8510	0.145
	Rear axle	6744	0.130
Loaded	Front axle	5812	0.137
	Rear axle	21 018	0.182

Table 7 Tyre contact area – data coincidence

Source	Calculation equation number	Data coincidence, %
Measured values		100
Schwanghart (1990)	*(21)*	92
Grechenko (1995)	*(22)*	50
Lyasko (1994)	*(23)*	23
Febo (1987)	*(24)*	49
Komandi(1990)	*(25)*	86
Dwyer (1984)	*(26)*	65

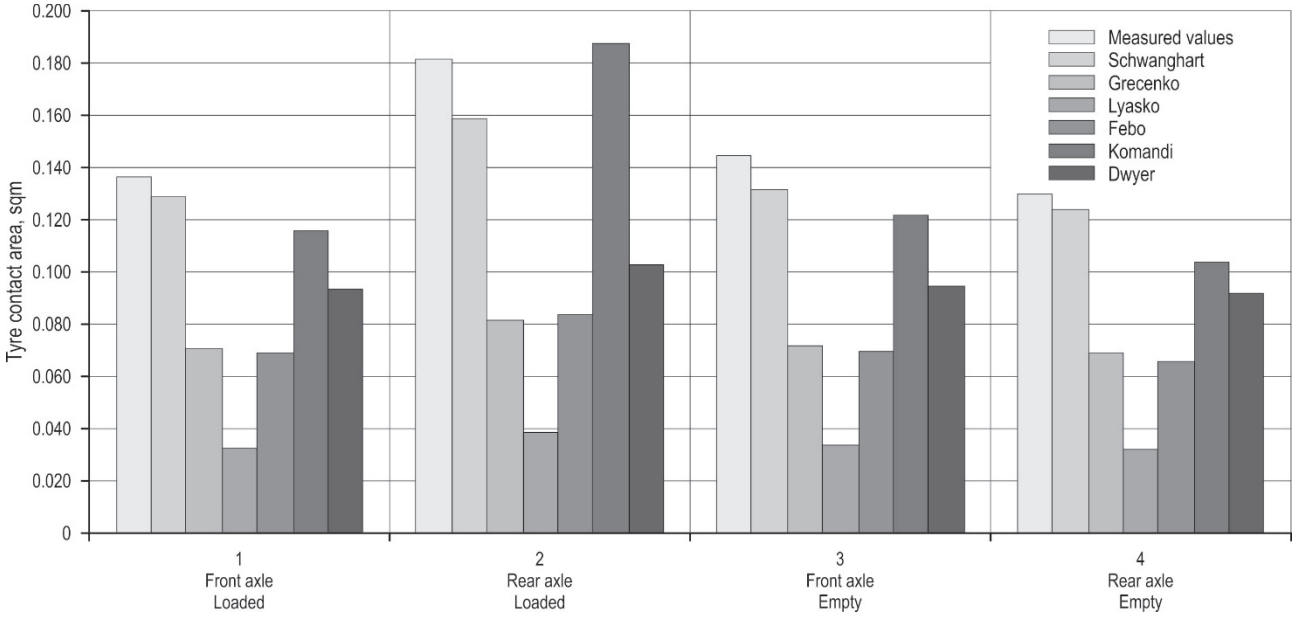

Fig. 7 Tyre/ground contact area – calculated and measured values

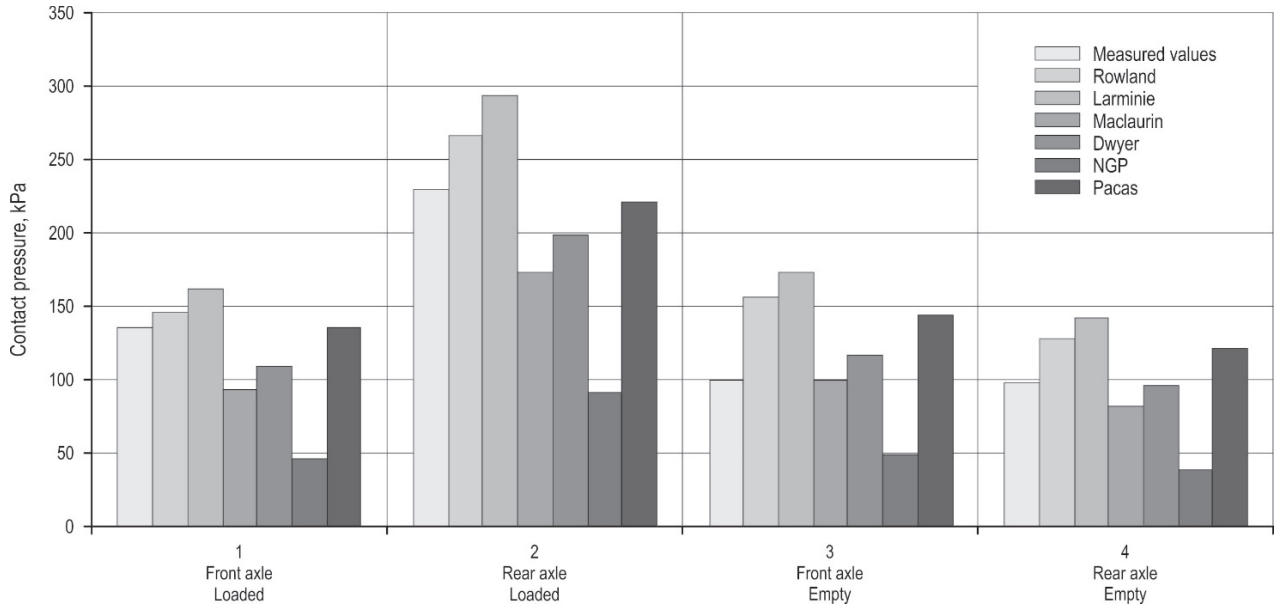

Fig. 8 Measured and calculated tyre contact pressures

The comparison of the agreement of the calculated and measured values, presented in Table 7 and in Fig. 7, show that the best suiting formulas for the calculation of the ground contact area of the tyre Mitas D FOREST 400/60–15.5 are those by Schwanghart (21) – coincidence of 92% and Komandi (25) – coincidence of 86%. Eq. (21) is used in the following calculations of tyre contact pressure.

4.3 Tyre Contact Pressure

Fig. 8 presents the measured and calculated tyre contact pressures. The contact pressures were measured and calculated for the front and rear axle of the empty and loaded machine. The coincidence between measured and calculated contact pressures is presented in Table 8.

The calculation equations give values from 45 to 160 kPa for front axle empty and from 93 to 290 kPa for rear axle loaded. The NGP (2) eq. seems to give very low values, while contact pressure calculated by the Larminie (4) and Rowland (3) eq. are slightly higher.

Eq. (5-Maclaurin) and (6-Dwyer) exhibit a relatively good agreement with the measured data also at the given static load. Eq. (1-Pacas) shows a similarly good agreement (81%) at the given dynamic load.

4.4 Dynamic load

The diagram in Fig. 9 presents the measured static load and calculated dynamic load of the wheels of front and rear axles. Horizontal lines represent permitted

Table 8 Tyre contact pressure – data coincidence

Source	Calculation equation number	Data coincidence, %
Measured values		100
Pacas (1990)	*(1)*	81
NGP	*(2)*	15
MMP Rowland (1972)	*(3)*	67
MMP Larminie (1988)	*(4)*	48
MMP Maclaurin (1997)	*(5)*	71
Dwyer (1984)	*(6)*	80

wheel load at various inflation pressures. It follows from the diagram that the dynamic load represents a multiple value of its static equivalent. Comparing the dynamic and the permitted load values, it can be concluded that, during the machine travel across the rugged terrain, the tyre experiences a short-term overloading beyond the tolerable limit. In addition, there is also the influence of reduced pressure in the tyre, which increases the tyre capacity of absorbing shock loads and hence partly reduces the level of dynamic load.

The static/dynamic load ratio, characterized by the dynamic coefficient β, is an important parameter in the machine design. It represents a load increase, to which the dimensions of all machine parts exposed to load during the machine travel (namely parts of chassis) are

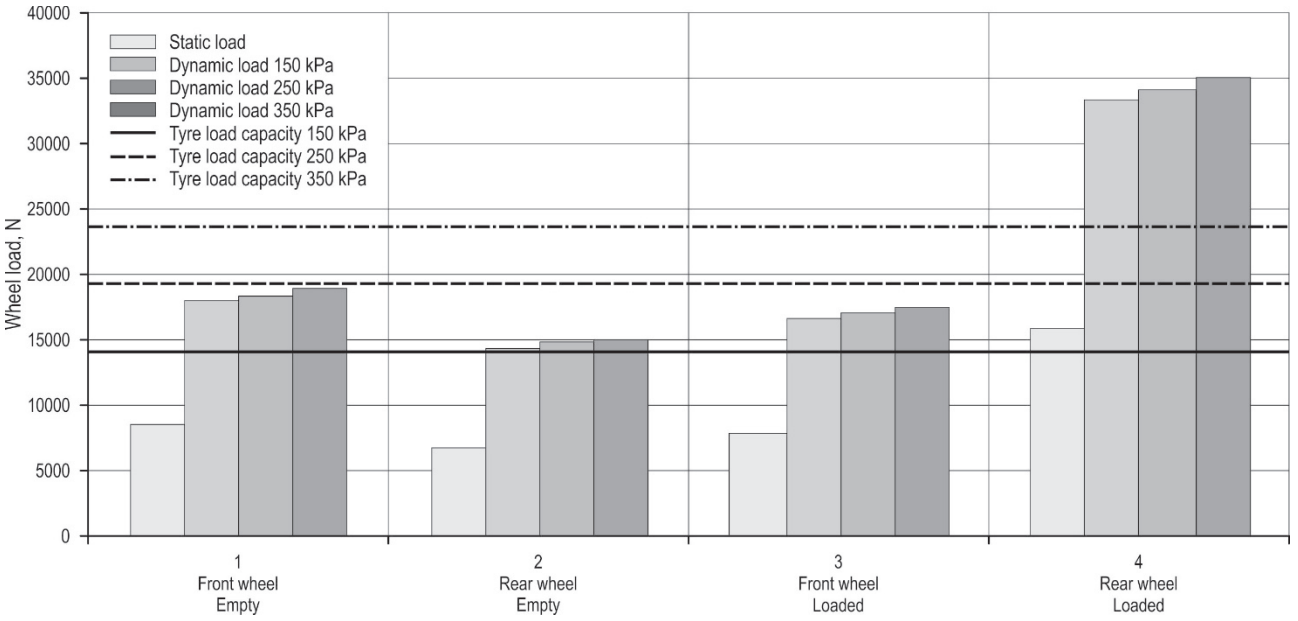

Fig. 9 Static and dynamic wheel load

to be accommodated. It also has great significance in wear calculations and in establishing the service life of machine parts. The size of the dynamic coefficient is determined through estimate according to required technical conditions of machine operation and based on measuring axle load in the machines of similar class. For example, in trucks moving on the road, $\beta = 1.2 \div 1.8$, while in military vehicles moving across the terrain at high speed, $\beta = 3.6 \div 4.0$. The results of calculations presented in the diagram (Fig. 8) indicate that the dynamic coefficient of a forest machine working in the field may reach values $\beta = 2.4 \div 2.6$.

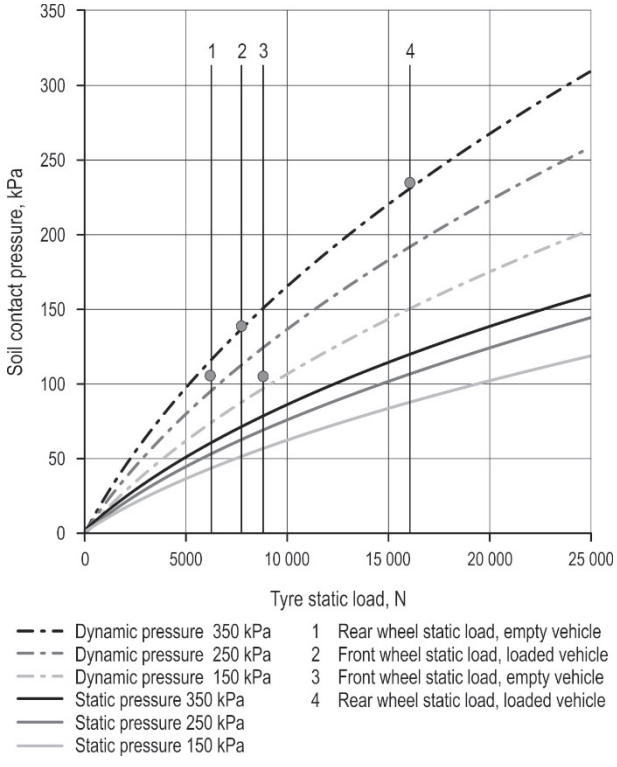

Fig. 10 Contact ground pressure caused by the tyre

The diagram in Fig. 10 shows the size of contact pressures at static and dynamic loads calculated according to the procedure for establishing dynamic pressures presented in Fig. 3. Horizontal lines in the diagram represent the contact pressure at the maximum tyre load for 3 levels of inflation pressure. Vertical lines in the diagram represent the level of calculated dynamic load on the front and rear axles in the empty and loaded machine. Values of contact pressures measured under the passing machine with tyres inflated to 350 kPa are illustrated as dots at the vertical lines of the diagram.

The diagram shows that dynamic contact pressures are by 1.6–2 times higher than contact ground pressures caused by the static load. Since the difference is decreasing with the decreasing tyre inflation pressure (2 times at 350 kPa, 1.6 times at 150 kPa), softer tyres have a higher capacity for reducing the shock load.

The reduced air pressure in tyres affects the size of dynamic pressures at several levels. The reduced pressure increases the tyre capacity to reduce the shock

load, which reduces the dynamic impact of the machine on the soil environment. The tyre with a lower pressure has a larger contact area, which reflects in a lower contact ground pressure.

In spite of the favourable effects of machine travel with the reduced tyre pressure on the soil, it is necessary to take into account the permitted tyre load in selecting the tyre pressure. This particularly applies to forwarders, where the load on the rear axle changes depending on whether the machine is loaded or empty. To prevent damage to tyres and to extend their service life, machine operators usually inflate them to the maximum prescribed pressure without considering environmental consequences.

In practice, it often happens that damage occurs to the sidewall of the tyre during the travel of machine with underinflated tyres, or a branch gets between the tyre bead and the wheel rim edge. Internal pressure in the tyre is too low to press the tyre to the wheel rim, which can even result in tyre spinning on the wheel rim at a powerful wheel engagement or in tyre slipping under the influence of lateral forces on the slope and at turning.

One of the methods to solve the problem is using a split rim with the BEAD LOCK ring in the wheel assembly (Fig. 11), which can provide additional thrust of tyre bead to the wheel rim even at a lower pressure. A similar principle with the RUN FLAT insert in wheels is used in military vehicles with the standard built-in central tyre inflation system or in vehicles transporting VIPs. A vehicle with the mounted BEAD LOCK rings is capable of moving over a certain distance even with the deflated tyre, e.g. in a difficult terrain or on low carrying capacity soils.

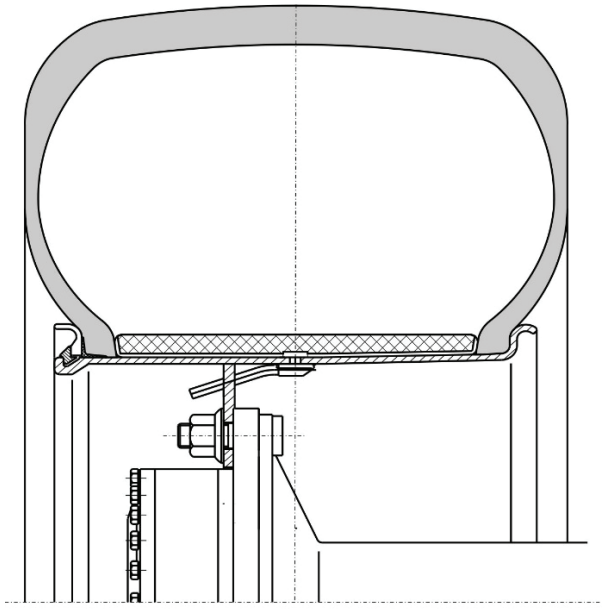

Fig. 11 BEAD LOCK ring

A disadvantage of this solution is a high price of the complete wheel and complex assembly. The ring is manufactured at a width higher than the inner size of the assembled tyre in order to generate pre-stress between the ring and the tyre walls. At assembling the wheel, it is necessary to press down the locking ring of the wheel rim and lock it in this position by the safety ring. Since a special fixture is used for this purpose, tyre replacement in the field is not possible.

Despite the above-mentioned disadvantages, it should be verified whether it is possible to use wheels with the BEAD LOCK ring in the operation of forest machines and to investigate their loading impact on the soil at driving with underinflated tyres.

5. Conclusion

This paper presents the method of determining contact ground pressures based on axle loads and machine travel speed. Calculation results and their comparison with the measured values show that this method of establishing the dynamic pressures can be an alternative to calculation models based on already applied WES and MMP methods. In the future, further tests will be needed to verify this calculation procedure also in the machines of higher load-carrying capacity class with different inflation pressures and travel speeds.

Acknowledgement

This paper was created as a part of the project TAČR Alfa TA04020087 »Development and manufacture of variable forwarder with the focus on ecological cleanliness of operations and effective processing of biomass in forestry«.

6. References

Alakukku, L., 1999: Subsoil compaction due to wheel traffic. Agricultural Science in Finland 8(4–5): 333–351.

Burt, E.C., Wood, R.K., Bailey, A.C., 1992: Some comparisons of average to peak soil tyre contact pressures. Trans. ASAE 35: 401–404.

Dwyer, M.J., 1984: Tractive performance of wheeled vehicles. Journal of Terramechanics 21(1):19–34.

Greacen, E.L., Sands, R., 1980: Compaction of forest soils. A review. Australian Journal of Soil Research 18(2): 163–189.

Grecenko, A., 1995: Tyre footprint area on hard ground computed from catalogue value. Journal of Terramechanics 32(6): 325–333.

Haas, H., 1994: Off-Road Tyres with Emergency Capabilities. Proceedings of the 6th ISTVS Conference, Vienna, 9/1994, 696–706.

Hallonborg, U., 1996: Super ellipse as tyre-ground contact area. Journal of Terramechanics 33(3): 125–132.

Jourgholami, M., Soltanpour, S., Etehadi, A.M., Zenner, E.K., 2014: Influence of slope on physical soil disturbance due to farm tractor forwarding in a Hyrcanian forest of northern Iran. iForest 7(5): 342–348.

Larminie, J.C., 1992: Modifications to the mean maximum pressure system. Journal of Terramechanics 29(2): 239–255.

Lysne, D.H., Burditt, A.L., 1983: Theoretical ground pressure distributions of log skidders (forest equipment). Trans. ASAE 26: 1327–1331.

Lyasko, M.I., 1994: The determination of deflection and contact characteristics of a pneumatic tire on a rigid surface. Journal of Terramechanics 31(4): 239–242.

Maclaurin, E.B., 1990: The use of mobility numbers to describe the in-field tractive performance of pneumatic tyres. Proceedings of the 10th ISTVS Conference, Kobe, 8/1990, 177–186.

Neruda, J., Ulrich, R., Kupčák, V., Slodičák, M., Zemánek, T., 2013: Harvestorové technologie lesní těžby Mendelova univerzita v Brně. ISBN 978-80-7375-842-4, 166 p.

Pacas, B., 1983: Teorie stavebních stroju. Vysoké učení technické v Brně. Publication Nr. 411-33363, 244 p.

Partington, M., Ryans, M., 2010: Understanding the nominal ground pressure of forestry equipment. FPInnovations, 12(5): 1–8.

Peng, C., Cowell, P.A., Chisholm, C.J., Lines, J.A., 1994: Lateral tyre dynamic characteristics. Journal of Terramechnics 31(6): 395–414.

Poršinsky, T., Stankić, I., Bosner, A., 2011: Ecoefficient Timber Forwarding Based on Nominal Ground Pressure Analysis. Croatian Journal of Forest Engineering 32(1): 345–356.

Rowland, D., 1972: Tracked vehicle ground pressure and its effect on soft ground performance. Proceedings of the 4th ISTVS Conference, April, Stockholm, Sweden, 353–384.

Saarilahti, M., 2002: Soil interaction model. University of Helsinki, Department of Forest Resource Management, Np. QLK5-1999-00991, 86 p.

Saarilahti, M., Anttila, T., 1999: Rut depth model for timber transport on moraine soils. Proceedings of the 13th ISTVS Conference, September 1999, Munich, Germany, 29–37.

Schwanghart, H., 1990: Measurement of contact area, contact pressure and compaction under tires in soft soil. Proceedings of the 10th ISTVS Conference, August, Kobe, Japan, 193–204.

Zahradníček, R., Semrád, K., 2007: Pružnosť a pevnosť II. Košice, TU, LF, 144 p.

Zemánek, T., Neruda. J., Ulrich, R., 2015: Okamžité tlaky v pude vyvozované přejezdy lesní techniky. Lesnictví. In Mobilné energetické prostriedky – hydraulika – životné prostredie – ergonómia mobilných strojov, Zvolen, Technická univerzita vo Zvolene, 171–178.

Authors' addresses:

Milan Marušiak, MSc. *
e-mail: milan.marusiak@gmail.com
Prof. Jindřich Neruda, PhD.
e-mail: neruda@mendelu.cz
University in Brno
Zemědělská 3
613 00 Brno
CZECH REPUBLIC

*Corresponding author

Received: June 18, 2017
Accepted: December 17, 2017